

Chapter 1

Introduction

Particle physics deals with the study of the basic constituents of matter and the forces governing the interactions among them. The Standard Model (SM) is the most accepted theory describing the nature and properties of the fundamental particles and their interactions. The elementary particles leptons and quarks, known as fermions, interact through the exchange of the gauge bosons. The gauge bosons acquire masses in the process of electroweak symmetry breaking whereas the masses of the fermions are generated through Yukawa interactions with the field associated to the scalar Higgs boson. The gauge bosons are the mediators of the four fundamental forces of interaction existing in nature : the electromagnetic force, the strong force, the weak force and the gravitational force. Quantum Chromodynamics (QCD) is the theory of the strong interactions between the quarks mediated by the massless gluons. The quarks and gluons, together known as partons, have a peculiar property of “color” charge. Due to confinement property of QCD, the quarks cannot exist freely in nature but bind themselves into colorless particles called hadrons such as protons and neutrons together known as nucleons, pions etc. The structure and the properties of sub-atomic particles can be explored by first accelerating them using particle accelerators and then colliding at very high energies. The end products of these collisions are recorded in the ~~real~~ particle detectors constituting the real data.

*slang
measurements?*

Vorlesung
 $\text{pp} \rightarrow i\text{jets} + X$, is proportional to α_s^i . The study of inclusive jet cross-sections in terms of jet transverse momentum p_T and rapidity y is very important because it provides the essential information about the PDFs and the precise measurement of α_s . Also the ratio of cross-sections given by Eq. 1.1 is proportional to the QCD coupling constant α_s and hence can be used to determine the value of α_s .

$$R_{mn} = \frac{\sigma_{m-jet}}{\sigma_{n-jet}} \propto \alpha_s^{m-n} \quad (1.1)$$

Instead of studying inclusive cross-sections, the cross-section ratio is more useful because of the partial or complete cancellation of many theoretical and experimental uncertainties in the ratio. The CMS Collaboration has previously measured the ratio of the inclusive 3-jet cross-section to that of the inclusive 2-jet as a function of the average transverse momentum, $\langle p_{T1,2} \rangle$, of the two leading jets in the event at 7 TeV [1]. This study leads to an extraction of $\alpha_s(M_Z) = 0.1148 \pm 0.0055$, where the dominant uncertainty stems from the estimation of higher-order corrections to the next-to-leading order (NLO) prediction. In this thesis, a measurement of inclusive 2-jet and 3-jet event cross-sections as well as ratio of 3-jet event cross-section over 2-jet R_{32} , is performed using an event sample collected during 2012 by the CMS experiment at the LHC and corresponding to an integrated luminosity of 19.7 fb^{-1} of pp collisions at a center-of-mass energy of 8 TeV. The event scale is chosen to be the average transverse momentum of the two leading jets, referred to as $H_{T,2}/2$

*Unclear:
 It is predicted
 if known
 at one
 scale, e.g. M_Z*
 in this thesis. The strength of the strong force, α_s at a given energy scale Q is not predicted and has to be extracted from the experiment. Hence, the value of the strong coupling constant at the scale of the Z boson mass $\alpha_s(M_Z)$ is extracted from the measurements performed in this thesis. The value of α_s depends on the energy scale Q and it decreases with the increase of Q scale. The running of α_s with scale Q is also studied and compared with other CMS measurements as well as results from different experiments. This checks the consistency with QCD via the

Chapter 7 describes the method to extract the strong coupling constant at the scale of mass of Z boson $\alpha_s(M_Z)$ from the measurements of differential inclusive multijet cross-sections and the cross-section ratio R_{32} . Also, the running of α_S with energy scale Q is presented along with the previous measurements from different experiments.

Chapter 8 summarizes the results and conclusions of the work done in this thesis.

Chapter 9 mentions the participation in other hardware and software activities.

Chapter 2

Theoretical Background

Since 1930s, many theories and discoveries in particle physics have revealed the fundamental structure of matter. The matter is made up of fundamental particles and their interactions are mediated by four fundamental forces [2]. The theoretical models describe all the phenomena of particle physics as well as predict the properties of particles. These models must be either confirmed experimentally or totally excluded giving hints of new physics. This interplay between experimental discoveries and the corresponding theoretical predictions leads to a theoretical model called Standard Model, which describes the fundamental particles and their interactions. The world's most powerful particle accelerators and detectors are used by physicists to test the predictions and limits of the Standard Model where it has successfully explained almost all experimental results. This chapter describes the Standard Model with main focus on the theory of strong interactions called Quantum Chromodynamics and its features which serve as the theoretical base of this thesis.

maybe? strive to describe, masses are not predicted

2.1 Standard Model

The Standard Model (SM) of particle physics [3–5] was developed in 1970s. It is a mathematical framework which describes the nature and properties of the funda-

Depending on how the fermions interact, these are classified into two categories - leptons (ℓ) and quarks (q). The leptons are of six types : electron (e), muon (μ) and tau (τ) with electric charge $Q = \pm 1$ ⁴ and the corresponding neutrinos : electron neutrino (ν_e), muon neutrino (ν_μ) and tau neutrino (ν_τ) having electric charge $Q = 0$. The quarks exist in six “flavors” : up (u), down (d), strange (s), charm (c), bottom (b) and top (t). u , c and t carry electric charge $Q = \pm \frac{2}{3}$ whereas d , s and b carry $Q = \pm \frac{1}{3}$. The quarks and leptons are categorized into three generations. The first generation has the lightest and the most stable particles whereas the heavier and less stable particles belong to the second and third generations.

The elementary bosons have integral spin and obey the Bose-Einstein statistics. These are further of two types : gauge bosons having non-zero integral spin and a scalar boson with zero spin. The gauge bosons are the force carriers which mediate the electromagnetic, strong, weak and gravitational forces. Every interaction involves the exchange of a gauge boson : the massless photon (γ) for the electromagnetic force, massless gluons (g) for the strong force, massive W^\pm and Z for the weak force and the graviton (not yet found) for the gravitational force. However, the gravitational force has not been incorporated into SM yet. Along with this, the existence of dark matter or dark energy and the matter-antimatter asymmetry are still missing pieces in the SM. The interaction between fundamental particles acts because of some peculiar property of the particles - charge for the electromagnetic force, color for the strong force and flavor for the weak force. *Usually Beyond SM.*

In the SM, the forces of interaction except gravity are unified into one quantum field theory [6], known as Grand Unified Theory (GUT) [7–9]. The SM framework based on quantum field theories is described by $SU(3)_C \otimes SU(2)_L \otimes U(1)_Y$ gauge symmetry where C stands for the color charge, L for weak isospin and Y for hypercharge. Here $SU(3)_C$, $SU(2)_L$ and $U(1)_Y$ terms give rise to strong, weak and

*Undefined
 $Y = ?$
Where is Q^3 ?*

⁴ all charges are expressed in units of elementary charge e

Define together with $t=c=1$?

Similar

has a same role as the electric charge in electromagnetic interactions. However, the mediator of electromagnetic interactions i.e. the photon itself does not carry any electric charge whereas the gluon itself carry color charge. This allows the self coupling of gluons and hence makes the theory non-abelian. Both the quarks and gluons carry three types of color charges : red (r), green (g) and blue (b), and three types of anti-color charges : anti-red (\bar{r}), anti-green (\bar{g}) and anti-blue (\bar{b}). The quarks carry a single color charge whereas gluons carry a combination of color charges. There are nine eigen states of gluons but one of them $\frac{1}{\sqrt{3}}(r\bar{r} + g\bar{g} + b\bar{b})$ is a totally symmetric color singlet which has no net color charge and does not take part in interaction.

The remaining eight eigen states of the gluons are :

$$r\bar{b}, r\bar{g}, g\bar{r}, g\bar{b}, b\bar{g}, b\bar{r}, \frac{1}{\sqrt{2}}(r\bar{r} - b\bar{b}), \frac{1}{\sqrt{6}}(r\bar{r} + b\bar{b} - 2g\bar{g}) \quad (2.1)$$

The dynamics of the quarks and gluons are controlled by the gauge invariant QCD Lagrangian \mathcal{L}_{QCD} which is composed of four terms as :

$$\mathcal{L}_{QCD} = \underbrace{-\frac{1}{4}F_{\mu\nu}^A F_A^{\mu\nu}}_{\mathcal{L}_{gluons}} + \underbrace{\sum_{flavors} \bar{q}_a (i\gamma^\mu (D_\mu)_{ab} - m_q) q_b}_{\mathcal{L}_{quarks}} + \mathcal{L}_{gauge} + \mathcal{L}_{ghost} \quad (2.2)$$

where \mathcal{L}_{gluons} describes the kinetic term of the gluon fields A_μ^A ; \mathcal{L}_{quarks} defines the interaction between spin- $\frac{1}{2}$ quark fields q_a of mass m_q and spin-1 gluon fields A_μ^A summing over all presently known six flavors of quarks; \mathcal{L}_{gauge} describes the chosen gauge and \mathcal{L}_{ghost} is the so-called ghost term required to treat the degeneracy of equivalent gauge field configurations in non-abelian gauge theories. In Eq. 2.2, the Greek letters $\mu, \nu, \dots \in \{0,1,2,3\}$ are the space-time indices; $a,b,c \in \{1,2,3\}$ and $A,B,C \in \{1,\dots,8\}$ are the indices of the triplet and octet representations, respectively,

color

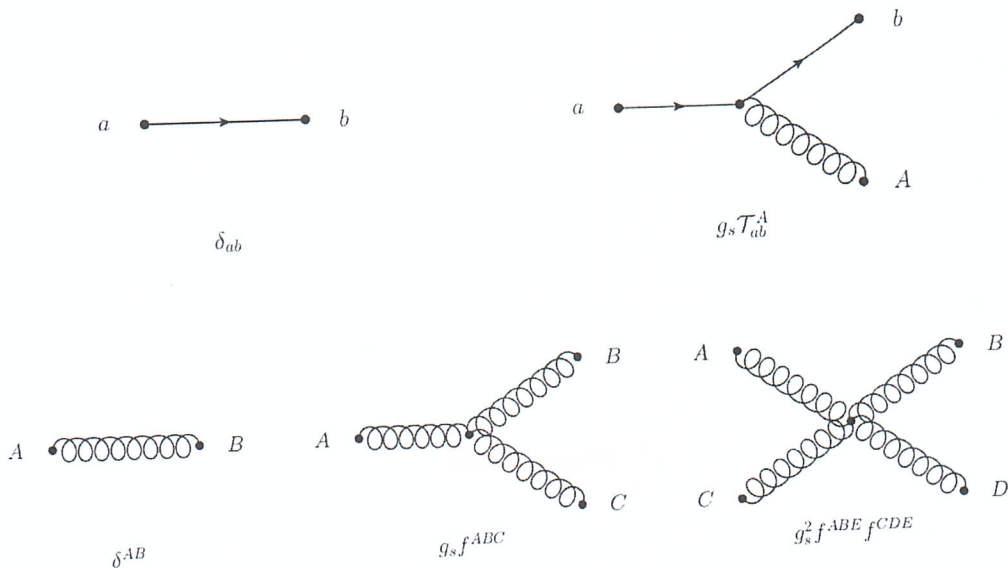


Figure 2.2: The fundamental Feynman rules of a free quark-field term (top left), cubic quark-gluon interaction term (top right), free gluon-field term (bottom left), quartic gluon self-interaction term (bottom middle) and quartic gluon self-interaction term (bottom right). Taken from [17].

is given by

$$\mathcal{L}_{gauge} = -\frac{1}{2\xi} (\partial^\mu \mathcal{A}_\mu^A)^2 \quad (2.6)$$

where ξ may be any finite constant. This choice fixes the class of covariant gauges with ξ as the gauge parameter. As QCD is non-abelian, the gauge fixing term must be supplemented by a ghost Lagrangian as

$$\mathcal{L}_{ghost} = \partial_\alpha \eta^{A\dagger} (D_{AB}^\mu \eta^B) \quad (2.7)$$

where η^A is a complex scalar field which obeys Fermi-Dirac statistics. The ghost fields cancel unphysical degrees of freedom arising due to use of covariant gauges. This completes the QCD Lagrangian shown in Eq. 2.2.

The strength of an interaction is given by a fundamental parameter called the coupling constant α . In QED, the coupling constant $\alpha_e = e^2/4\pi = 1/137$ is constant. In contrast to this, in QCD, the coupling constant $\alpha_S(Q) = g_s^2/4\pi$ is

No, also α_e is running because of renormalisation!

e.g.: $\alpha_e(M_Z) \approx 1/128$

to that process. For a given Feynman diagram, the power of α_s is determined by the number of vertices associated with quark-gluon or gluon-gluon interactions. A leading order (LO) prediction sums over only the lowest-order contribution whereas next-to-leading order (NLO) includes terms with ~~the additional powers~~^{one} of α_s . The next-to-next-to-leading order (NNLO) includes emission of another gluon or a virtual gluon loop. The different order of the QCD processes are shown in Fig. 2.3. The calculations become complex with the loop diagrams where the momenta of

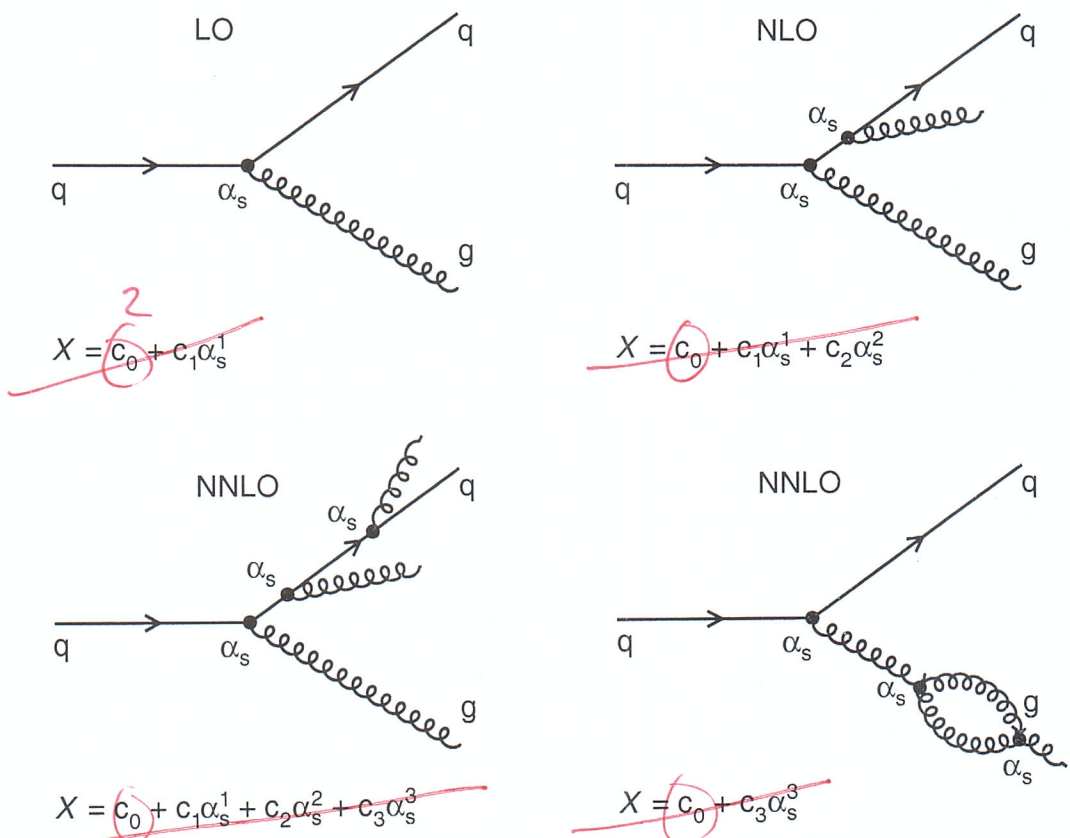


Figure 2.3: ~~The~~⁵ Feynman diagrams⁵ of leading-order (LO), next-to-leading order (NLO) and next-to-next-to-leading order (NNLO) processes in quantum chromodynamics along with the perturbative expansion of any observable X in powers of the strong coupling constant α_s . At each successive step in perturbation series, the emission of an additional gluon take place.

Power counting not clear. Better show concrete diagrams for your case. See after page 31!

the virtual particles in a loop are not fully constrained by four-momentum conservation and the associated integrals are divergent. Such ultraviolet (UV) divergences

⁵Drawn using ROOT

By setting the renormalization scale equal to the physical scale i.e. $\mu^2 = Q^2$, $X(1, \alpha_s(Q))$ is a solution to above equation. Q -dependence of ~~the~~ X is only from the renormalization of the theory which is present in the ~~classical~~? theory. Hence measuring the Q -dependence of X will directly probe the quantum structure of the theory. The β function in QCD has a perturbative expansion as :

$$\beta(\alpha_s) = -\alpha_s^2 \left(b_0 + b_1 \alpha_s + b_2 \alpha_s^2 + \mathcal{O}(\alpha_s^3) \right) \quad (2.11)$$

where b_n is the $n+1$ -loop β -function coefficients giving the dependence of the coupling on the energy scale Q . In the modified minimal subtraction ($\overline{\text{MS}}$) scheme [19, 20], the beta coefficient functions have following values :

$$b_0 = \frac{33 - 2n_f}{12\pi}, \quad b_1 = \frac{153 - 19n_f}{24\pi^2}, \quad b_2 = \frac{77139 - 15099n_f + 325n_f^2}{3456\pi^3} \quad (2.12)$$

where n_f is the number of quark flavours with masses $m_q < \mu_r$. On integration of Eq. 2.11, the energy dependence of α_s is yielded. Neglecting the higher orders, the first order solution of RGE is :

$$\alpha_s(\mu_r^2) = \frac{1}{b_0 \ln(\mu_r^2/\Lambda_{QCD}^2)} \quad (2.13)$$

where Λ_{QCD} is the constant of integration. The perturbative coupling becomes large at the scale Λ_{QCD} and the perturbative series diverge. With $b_0 > 0$, the coupling becomes weaker at higher scales Q , i.e. the effective color charge is small at small distances or large energies. This allows the quarks to behave as free particles within the hadron, leading to the property called asymptotic freedom. It is always convenient to express α_s at some fixed scale. Since some of the best measurements come from Z decays, it is common practise to determine the strong coupling at the $\overline{c^2}$.

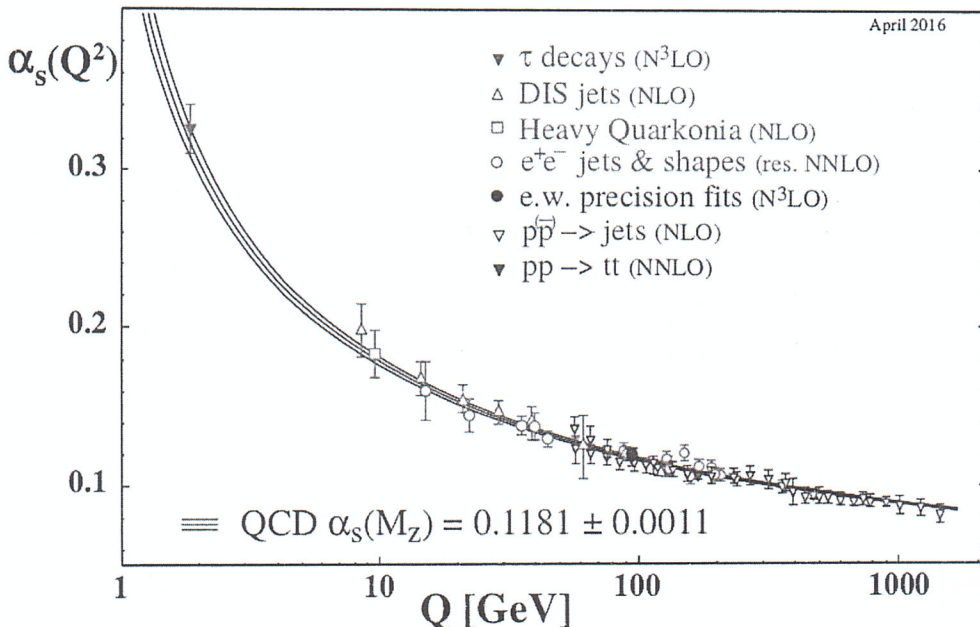


Figure 2.4: The different experimental measurements of the strong coupling constant α_S evolved at the energy scale Q are shown as a function of Q . These describe the running of the α_S up to the 1 TeV scale. Taken from [21].

final state?

specific process. In a hadronic collision, the perturbation theory is only valid at the parton-level but due to property of confinement at low energies, free partons cannot exist in nature. Only hadrons with a complex internal structure are available for the high energy collisions. Here, a factorization theorem of QCD [22] comes into play which allows the calculation of σ by separating into two parts : a short-distance partonic cross-section calculable with pQCD, and a non-perturbative long-distance part described by parton distribution functions $f_i(x, \mu_f)$ (PDFs). The PDFs describe the partonic content of the colliding hadrons and give the probability to find a parton i with momentum fraction x within a hadron. μ_f is a factorization scale which corresponds to the resolution with which the hadron is being probed. The particles which are emitted with transverse momenta $p_T > \mu_f$ are considered in the calculation of hard scattering perturbative coefficients. The particles emitted with $p_T < \mu_f$ are accounted for within the PDFs. Applying the factorization theorem

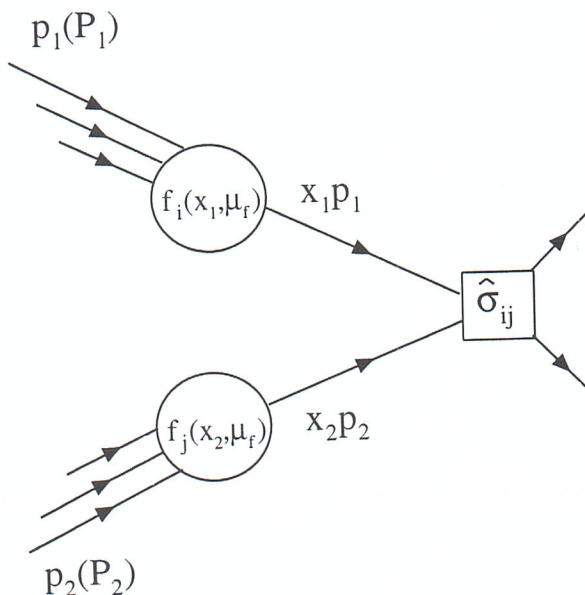


Figure 2.5: Schematic illustration⁶ of the factorization theorem in a collision of two protons P_1 and P_2 having momenta p_1 and p_2 , respectively. In a hard-scattering process at a scale Q^2 , the two partons x_1 and x_2 participate with momenta $x_1 p_1$ and $x_2 p_2$. The total cross-section is factorized into the hard scattering cross-section $\hat{\sigma}_{ij}$ calculable using perturbative quantum chromodynamics and the PDFs $f_i(x_1, \mu_f)$ and $f_j(x_2, \mu_f)$ with factorization scale μ_f . p QCD

2.3.1 Parton Shower and Hadronization

The partons involved in a hard scattering process get accelerated due to large momentum transfers. These accelerated partons emit QCD radiation in the form of gluons with successively lower energy. Unlike the uncharged photons in QED, the gluons themselves carry color charge and hence also emit further gluons. The emitted gluons in turn split into $q\bar{q}$ pairs. This successive emission of partons leads to a parton shower. In a parton shower, the main contribution is by the collinear parton splitting and the soft gluon emissions. The parton showers mimic the effect of higher-order corrections to the hard process. These cannot be calculated exactly and are taken into account using the parton shower approximation. The two incom-

*Unity
color
vs.
colour
usage.*

⁶Drawn using ROOT

A consequence

Due to this, the potential energy of the string grows at the expense of the kinetic energy of the quarks. As the potential energy becomes of the order of hadron masses, the string breaks at some point along its length, creating a new $q\bar{q}$ pair. The newly formed two string segments again stretch and break producing further $q\bar{q}$ pairs. This process of stretching and breaking continues until all the potential energy gets converted to $q\bar{q}$ pairs. This whole process is illustrated in Fig 2.6. The $q\bar{q}$ pairs then undergo hadronization due to confinement property. PYTHIA Monte Carlo generator uses the Lund string model.

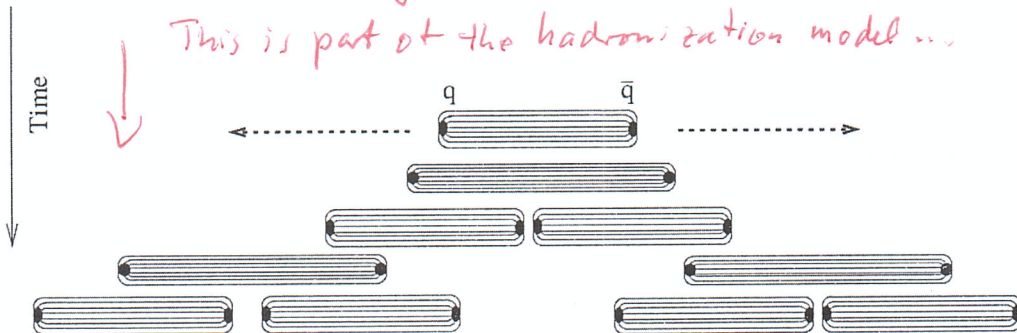


Figure 2.6: Illustration of the hadronization process in Lund string model⁸. When the quark q and anti-quark \bar{q} are pulled apart from each other, the potential energy of the gluonic string connecting the quarks increases. As it becomes of the order of hadron masses, the string breaks and a new $q\bar{q}$ pair is created. The breaking of string and creation of $q\bar{q}$ continues till all the potential energy gets converted to $q\bar{q}$ pairs which then get hadronized.

Cluster Model - The cluster model of hadronization [33, 34] is based on preconfinement property of QCD [35]. According to this property, at evolution scales Q_0 much less than the hard process scale Q , the partons produced in a shower are clustered in colourless groups with an invariant mass distribution, depending on nature of hard process and Q_0 , not on Q . This model contains two steps : firstly all gluons split into $q\bar{q}$ pairs at the end of the parton shower and in the second step, a new set of low-mass color-singlet clusters are obtained which decay into either secondary clusters or directly into hadrons. The generator HERWIG is based on the cluster

⁸Source : <http://inspirehep.net/record/806744>

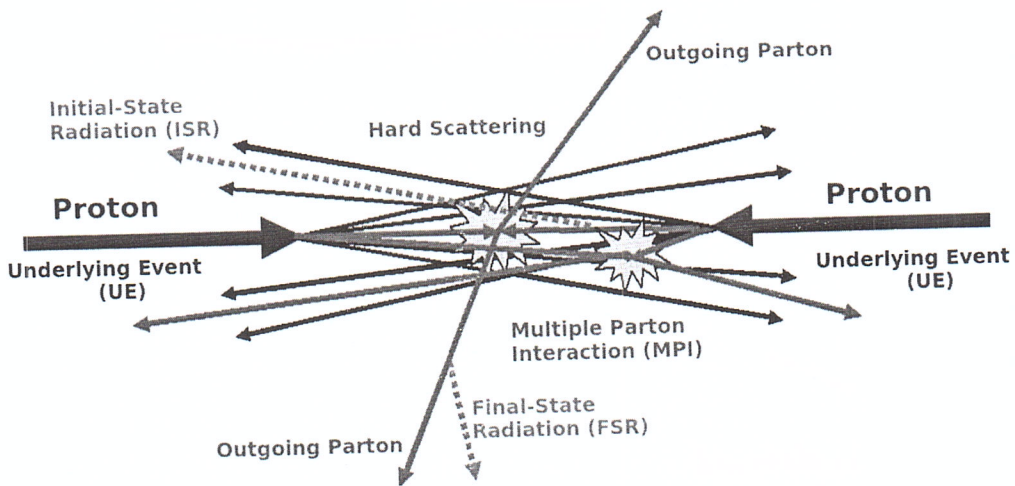


Figure 2.7: A proton-proton collision⁹ involving the main hard scattering process along with the low momentum transfer underlying event (UE) contributions coming from initial- and final-state radiations (ISR and FSR) complemented with multiple parton interactions (MPI) and collisions from leftover partons called beam remnants.

This is not the point! Only at low p_T ! Then jets are background. The real multijet is from $2 \rightarrow 3$, $2 \rightarrow 4$, ... proton reaction in QCD!

and also to reduce the uncertainties of the PDFs of proton. In LHC, the simplest jet production process is $2 \rightarrow 2$ scattering process at leading-order giving dijet events. But the partons originating from ISR, FSR or MPI can also hadronize to produce jets within the same further than 2 in a single proton-proton collision. This results in the production of multijet events. The investigation of inclusive multijet event cross-sections permits more elaborate tests of QCD. Also, a precise study of jet variables helps to understand the signal and background modelling for the new physics searches in hadronic final states. In this thesis, the inclusive multijet event cross-sections as well as the ratio of cross-sections are exploited to extract the value of strong coupling constant α_s . In the next section, we focus on the definition of a jet.

In your analysis the UE multijet events are cut out using $p_T > 100 \text{ GeV}$.

2.4 Jets

Jets [36] are the conical structures which group the hadrons into a single physics entity. Figure 2.8 shows the outgoing partons of the hard scattering process

⁹Source : The Energy Dependence of Min-Bias and the Underlying Event at CDF

ated with a jet algorithm which calculates the momentum assigned to the combined particles. A jet algorithm along with its parameters and a recombination scheme forms a “jet definition”. A jet definition [39] must be simple to implement in an experimental analysis as well as in the theoretical calculation. It should be defined at any order of perturbation theory and must yield finite cross-sections that is relatively intensive to hadronization. In addition to these requirements, a jet algorithm must be infrared and collinear (IRC) safe. Infrared safety is the property by which the addition of a soft emission i.e. addition of a soft gluon should not change or modify the number of hard jets found in an event. In an infrared unsafe algorithm, a soft gluon emission in the middle of two cone jets can lead to overlap of the two initial cones, as shown in Fig. 2.9 (top). This produces a single jet instead of initial

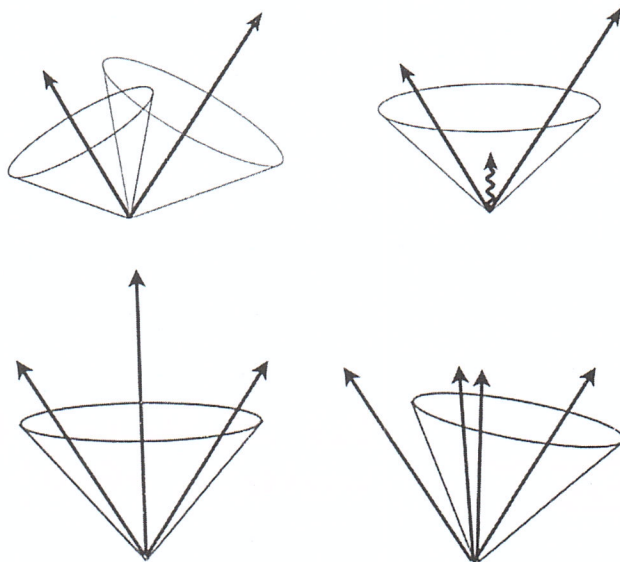


Figure 2.9: Top : Infrared unsafe behaviour of jet algorithm is illustrated where the presence of soft radiation between two jets may cause a merging of the jets that would not occur in the absence of the soft radiation. Bottom : Collinear unsafe behavior of jet algorithm is shown in which the number of jets change due to a collinear splitting¹⁰.

two jets resulting in the change of number of jets. Collinear safety is the property by virtue of which the collinear splitting i.e. replacement of one parton by two at

¹⁰Source : <http://inspirehep.net/record/1251416>

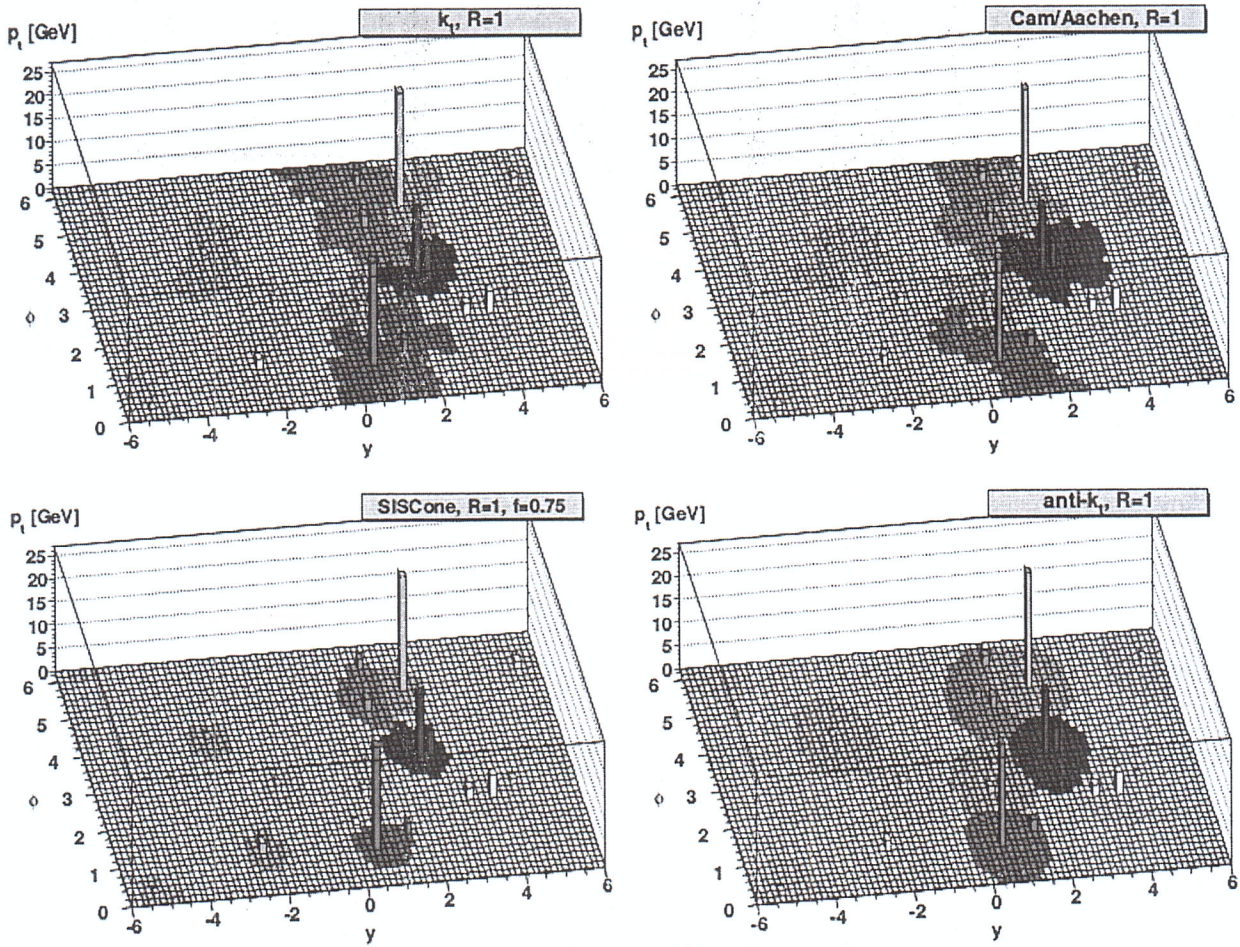


Figure 2.10: The clustering of particles, in $y\phi$ space at the parton level, into jets clustered with the k_t (top left), Cambridge/Aachen (top right), SIScone (bottom left) and anti- k_t (bottom right) algorithms with $R = 1$. The towers represent the jet p_T . The anti- k_t algorithm gives circular jets while the jets produced with other three algorithms have irregular shapes. Taken from [38].

corresponds to vector addition of four-momenta where the four-momenta of the jet is obtained by simply adding the four-momenta vector of merging particles.

The sequential clustering algorithms have ~~always~~^{traditionally} been favoured by theorists but not by experimentalists because of slow computational performance. However, the introduction of the FASTJET program [47] enhanced the speed of clustering algorithms and hence are preferred by experimentalists as well. This thesis studies the particles produced in proton-proton collisions by clustering them in to jets using

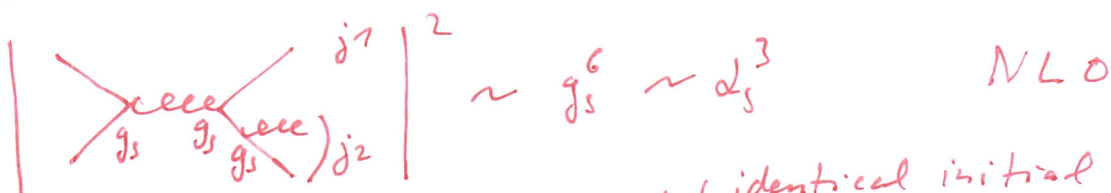
anti- k_t algorithm with distance parameter $R = 0.7$. These jets are observed in the Compact Muon Solenoid detector of the Large Hadron Collider, the details of which are discussed in the following chapter.

To Fig. 2.3

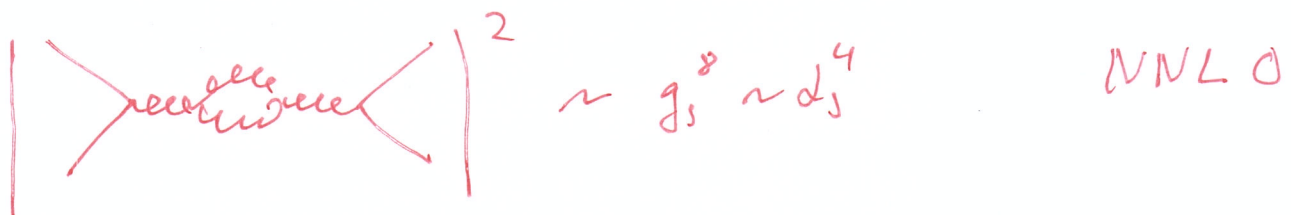
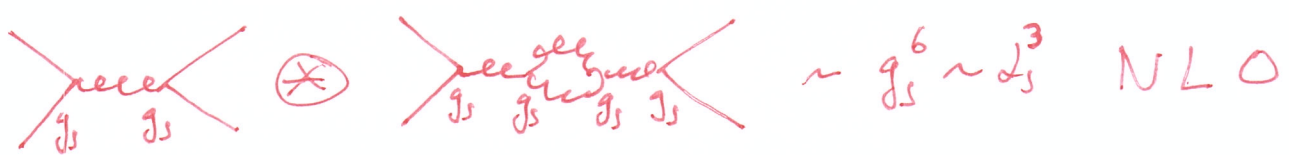
The bottom right diagram (loop) contributes to the NLO via interference!

The listed diagrams do not represent e.g. a scattering process:

~~PPF~~ parton + parton \rightarrow 2 + partons (e.g. $pp \rightarrow 2\text{jets} +$)
 $g_s^2 = 4\pi\alpha_s$



interference term! (identical initial & final state)



particle to the beam are calculated.

$$d_{ij} = \min(p_{Ti}^{2p}, p_{Tj}^{2p}) \frac{\Delta R_{ij}^2}{R^2}, \quad d_{iB} = p_{Ti}^{2p} \quad (2.18)$$

where $\Delta R_{ij}^2 = (\eta_i - \eta_j)^2 + (\phi_i - \phi_j)^2$

η_i η_j !

jet object

2. If $d_{ij} < d_{iB}$, then the particles i and j are merged into a new single particle k , summing four-momenta of two initial particles by recombination scheme and step 1 is repeated.
3. If $d_{iB} < d_{ij}$, particle i is declared as a final-state jet and the wave removed from the list.

This procedure continues until all particles get clustered into jets. The value of the parameter p defines the three different sequential algorithms having distinct properties. For $p = 1$, we have k_t algorithm [43, 44], $p = 0$ gives the Cambridge/Aachen (C/A) algorithm [45] whereas $p = -1$ defines the anti- k_T algorithm [46]. The k_t algorithm involves clustering of soft particles first resulting in an area that fluctuates considerably. This algorithm is susceptible to the underlying and pileup events. The C/A algorithm involves energy independent clusterings. Both k_t and C/A produce jets of irregular shapes. Instead of jet analysis, these are widely considered for studying the jet substructure. The anti- k_T algorithm tends to cluster hard particles first and produces more jets with circular regular shapes. It is less sensitive to underlying and pileup events. It is the most preferred algorithm for jet studies at the LHC. Figure 2.10 shows the clustering of same particles but using the different jet algorithms.

A jet algorithm must specify how to combine the momenta of different partons or particles going to be clustered into a jet. This is given by the recombination scheme. The most widely used recombination scheme is the E -scheme [40] which

the same place should not modify the number of jets formed in an event. This implies that the output of the jet algorithm should remain the same if the energy of a particle is distributed among two collinear particles. According to the collinear safety property, the two cases shown in Fig. 2.9 (bottom) should always produce a single jet. If an algorithm produces zero or two jets after collinear splitting, then it is not collinear safe. The jet algorithms can be classified mainly into two types :

Cone algorithms - In the iterative cone (IC) algorithm [40], the jet is defined as a cone with fixed radius R in $\eta\text{-}\phi$ space drawn around the highest energy seed. The relative distance (d) of all the particles is iteratively calculated and compared with R . If the calculated $d < R$, the considered particles are clustered together in a jet and the directions of the clustered particles give the direction of the jet. On the other side i.e. if $d > R$, the considered particles initiate two different jets. The algorithm iterates until the cone is stable which means that the direction of sum of momentum of all the particles is same as that of the center of cone. But IC algorithm is not IRC safe. There is another cone algorithm, Seedless Infrared-Safe cone (SIS-Cone) [41], which is an exact seedless i.e. does not rely on seed threshold and is IRC safe. This is a complex approach which tests the stability of all subsets of particles and has a complexity of $\mathcal{O}(N2^N)$ for N particles. But this algorithm is much slower and hence not preferred.

recombination

But it's the only cone
usable in pQCD!

Sequential algorithms - The sequential algorithms [42] cluster the particles by defining a distance between pairs of particles and recombine the pair of closest particles successively. This is collinear and infrared safe algorithm. It is possible for the jet cones to overlap such that one particle is contained in more than one jet but the sequential algorithm never assigns a particle to more than one jet. The sequential algorithm is based on transverse momentum p_T of the particles and follows the below procedure :

1. First the distance d_{ij} between two particles i and j and distance d_{iB} of the

in a proton-proton collision, undergoing fragmentation and hadronization processes and forming a conical jet with radius R. The jet structure was observed for the first time in hadron production of e^+e^- annihilation process at SLAC in 1975 [37]. The partons can not be measured directly by the experiments because they can not exist freely in nature. The information about the dynamics of the partons can be obtained indirectly from jets. The configurations of high-energy quarks and gluons at short distances are truly reflected in the energy and angular distributions of the jets. Hence the jets are important to study. To perform the clustering of particles, a certain set of rules are followed in the form of jet algorithms.

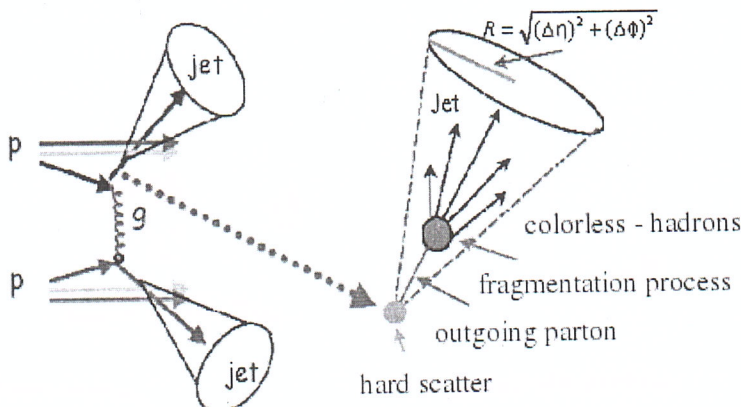


Figure 2.8: In a proton-proton collision, the outgoing partons of the hard scattering process undergo fragmentation and hadronization processes producing a shower of partons which get collimated into a conical jet with radius R.

2.4.1 Jet Algorithms

Jet algorithms [38] provide a set of rules which determine how the particles can be clustered into a jet. In a jet algorithm, usually one or more parameters are involved that indicate how close two particles must be for them to belong to the same jet. These parameters can either measure closeness in coordinate space (cone algorithms) or in momentum space (sequential algorithms). The jet algorithms are applicable on parton, particle and ~~calorimeter~~ levels. A recombination scheme is always associated with the ~~detector~~.

fragmentation model. However, this model has problems in dealing with the decay of very massive clusters. — You don't discuss problems of the string model either ...

2.3.2 Underlying Event

Due to the composite nature of the protons, their collisions are not clean events.

The event structure is significantly more complex than that of the lepton collisions.

The final states of the collisions involve the multi-particle calculations. In a high energy proton-proton collisions, the underlying event (UE) includes the effects which are not coming from the primary hard scattering process. The UE includes the contributions from relatively small momentum transfer processes : initial and final-state radiations (ISR, FSR), leftover partons in the collisions called beam remnants and multiple parton interactions (MPI). Due to composite nature of proton, the remaining two partons which do not participate in a hard collision may also interact giving rise to multiple parton interactions. The UE induces an additional energy in an event which is not related to the main hard interaction. This acts as an unavoidable background which needs to be removed. Hence, it is very crucial to study and understand the UE. The UE activity increases with Q and the center-of-mass energy \sqrt{s} . Figure 2.7 shows the complex variety of processes taking place in a single proton-proton collision.

The bunch of hadrons, produced from hadronization of quarks and gluons, gets collimated in the form of "jets" with the direction towards the direction of the initial parton that originated them. The jets are the final structures observed experimentally in the detectors. These act as a bridge between the elementary quarks and gluons of QCD and the final hadrons produced in high energy collisions. Therefore, at large momentum transfer of the interacting partons, the jets and their observables are the best tools to test the predictions of perturbative QCD. Also, the jet production is sensitive to the strong coupling constant α_s . The precise knowledge of the jet production cross-section can help to extract the value of α_s .

If you define acronyms, you have to use them ...

Slang

✓ Yes.

ing partons, which are constituents of two colliding hadrons and taking part in hard scattering process, can also develop parton showers, commonly known as Initial-State Radiation (ISR). The initial partons produce showers till they collide to initiate the hard scattering process. The final outgoing partons produced from a hard scattering process can also undergo parton showering giving rise to Final-State Radiation (FSR). A parton shower terminates when the scale Q is below the hadronization scale ~ 1 GeV for QCD.

At the end of the shower, there is a decrease in the energy of partons due to successive emission of gluons. Due to this, the coupling constant of QCD α_s grows and QCD is not applicable any more. This leads to the confinement of colored quarks and gluons into the color-neutral composite particles called hadrons and this process is known as hadronization. The hadronization takes place at low momentum transfer and hence is non-perturbative in nature. Although no exact theory for hadronization is known, the different phenomenological models have been developed to simulate the hadronization process. The two main models implemented in Monte Carlo event generators to simulate the hadronization process are :

Lund String Model - In the Lund string model of hadronization [32], the highly energetic gluons are treated as field lines. Due to the gluon self-interaction, the gluons are attracted to each other forming a narrow tube or string of strong color field between a $q\bar{q}$ pair. This model is based on an observation that at distances greater than about a femtometre (fm)⁷, the potential energy $V(r)$ of colored quarks grows linearly with the increase in distance between them (r) as :

$$V(r) = \kappa r \quad (2.17)$$

where $\kappa \sim 1$ GeV/fm² is the tension of the string connecting the quarks. When the q and \bar{q} are pulled apart from each other move apart, the gluonic string stretches.

⁷ 1 femtometre = 1×10^{-15} metres

In a proton-proton collision, the cross-section of a hard scattering process can be written as :

$$\sigma_{P_1 P_2 \rightarrow X} = \sum_{i,j} \int dx_1 dx_2 f_{i,P_1}(x_1, \mu_f) f_{j,P_2}(x_2, \mu_f) \times \hat{\sigma}_{ij \rightarrow X} \left(x_1 p_1, x_2 p_2, \alpha(\mu_r^2), \frac{Q^2}{\mu_f^2} \right) \quad (2.16)$$

where f_i and f_j are the proton PDFs which depend on momentum fractions x_1 and x_2 of parent protons P_1 and P_2 respectively as well as on the factorization scale μ_f . The sum extends over all contributing initial-state parton flavours i, j . The cross-section for the production of final state X at parton level ($\hat{\sigma}_{ij}$) depends on the final state phase, the factorization scale μ_f and the renormalization scale μ_r . Figure. 2.5 illustrates the factorization into the PDFs and the hard scattering cross-section in a proton-proton collision.

The PDFs of the proton are a necessary input to almost all theory predictions of a proton-proton collision. The QCD does not predict the parton content of the proton. So the shapes of PDFs are determined in fits to experimental measurements of different experiments. The dependence of PDFs on μ_f is given by the Dokshitzer-Gribov-Lipatov-Altarelli-Parisi (DGLAP) [23–25] equations which use α_s and the RGE as inputs. The knowledge of proton PDFs mainly comes from the Deep-Inelastic Scattering (DIS) HERA, fixed-target and Tevatron data. The LHC data has a potential to improve constraints of the PDFs further as done in one of the recent CMS measurements [26]. There are several groups which determine the PDFs using various minimization methods, phenomenological approaches, and the strategies to estimate the uncertainties. The global PDFs are the CTEQ [27], MMHT [28], NNPDF [29], ABM [30] and HERAPDF [31] at LO, NLO and NNLO.

*not global
since only HERA data!*

scale of the Z boson mass $\alpha_s(M_Z)$. So, Eq. 2.13 can be expressed as :

$$\alpha_s(\mu_r, \alpha_s(M_Z)) = \frac{\alpha_s(M_Z)}{1 + \alpha_s(M_Z)b_0 \ln(\mu_r^2/M_z^2)} \quad (2.14)$$

Since α_s is ~~a~~ the free parameter of QCD theory, it ~~is always~~ extracted from ~~the~~ experimental measurements and evolved to the scale of the Z boson. According to Particle Data Group (PDG) [21], the current world average value of the strong coupling constant at the scale of mass of Z boson is $\alpha_s(M_Z) = 0.1181 \pm 0.0011$.

$$\alpha_s(M_Z) = 0.1181 \pm 0.0011 \quad (2.15)$$

This value is derived using data from deep inelastic scattering process, electron-positron annihilation processes, hadronic τ lepton decays, lattice QCD calculations and electroweak precision fits. The different experimental determinations of the strong coupling constant evolved at the scale Q are shown as a function of Q in Fig. 2.4 which describe the running of the α_s up to the 1 TeV scale.

2.3 Hadronic Collisions

At ~~a~~ large momentum transfer, the collision between two hadrons can be visualized as an interaction between their constituents - quarks and gluons. In this thesis, we are studying the proton-proton collisions taking place at the Large Hadron Collider (LHC). A proton is a complex composite particle consisting of three valence quarks (uud), gluons for the exchange of the strong force and the sea quarks. The sea quarks consist of quark-antiquark pairs coming into and out of existence rapidly and continuously due to gluon colour field splitting. In any collision, ~~one of the~~ ~~most important quantities~~ to evaluate is the cross-section (σ) of a certain process which gives the probability that the two hadrons interact and give rise to that

enter the calculations beyond LO either due to loop or vertex corrections. These are overcome by a procedure known as renormalization, described in next section. Apart from the UV divergences, the QCD also suffers from infrared and collinear divergences (IRC) due to the presence of massless gluons and neglected quark masses. These need to be handled in pQCD calculations. The observable to be studied must be IRC safe.

2.2.2 Renormalization and Running of the Strong Coupling

The renormalization is a mathematical procedure which allows the finite calculation of momenta integrals of virtual loop by removing UV divergences. It introduces a regulator for the infinities, the renormalization scale μ_r . At first, the divergences are regularized temporarily by introducing a cut-off to the loop momenta at μ_r scale. Then the free parameters of the Lagrangian, i.e. the coupling constant are redefined or renormalized to absorb the UV divergences. Due to this, both $\alpha_s(Q)$ and observable X become a function of μ_r . The exact dependence of $\alpha_s(\mu_r^2)$ on μ_r is described by the renormalization group equation (RGE) [18] which determines the running of $\alpha_s(\mu_r^2)$. According to RGE, the dependence of X on μ_r must cancel. Mathematically this can be expressed as :

$$\mu_r^2 \frac{d}{d\mu_r^2} X \left(\frac{Q^2}{\mu_r^2}, \alpha_s(\mu_r^2) \right) = \left(\mu_r^2 \frac{\partial}{\partial \mu_r^2} + \mu_r^2 \frac{\partial \alpha_s(\mu_r^2)}{\partial \mu_r^2} \frac{\partial}{\partial \alpha_s(\mu_r^2)} \right) X = 0 \quad (2.9)$$

Using beta function $\beta(\alpha_s) = \mu_r^2 \frac{\partial \alpha_s(\mu_r^2)}{\partial \mu_r^2}$, Eq. 2.9 can be re-written as

$$\left(\mu_r^2 \frac{\partial}{\partial \mu_r^2} + \beta(\alpha_s) \frac{\partial}{\partial \alpha_s(\mu_r^2)} \right) X = 0 \quad (2.10)$$

↙ Same for QED.

not constant and depends on the separation between the interacting particles. It increases with the increase in the distance or decrease in the energy scale Q . At large distances or low energies, the quarks can never be found as free particles but exit in color neutral bound states known as hadrons. Hadrons are of two types : baryons and mesons. According to the quark model [2] every (anti-)baryon is made up of three (anti-)quarks and every meson is made up of a quark-antiquark pair. When the colored partons within a hadron are pulled farther and farther apart, there is an increase in the strength of force between them. This results in creation of new quark-antiquark pairs making it impossible to liberate a free quark or gluon. This property of QCD is known as confinement according to which at low energy, the partons are forever bound into hadrons such as protons (uud), neutrons (udd) etc. Although the gluons are massless ~~but~~ the confinement leads to the finite range of the strong interactions. On the other hand, at small distances, the strength of coupling decreases. The quarks and gluons interact very weakly and behave as free particles. This property is known as asymptotic freedom. This indicates that perturbative theory is only applicable at high energies or small distances.

2.2.1 Perturbative Quantum Chromodynamics

At high energies, the property of asymptotic freedom allows a perturbative treatment in QCD calculations. In perturbative quantum chromodynamics (pQCD), any physical observable X such as cross-section of a scattering process, can be expanded as a perturbative series in terms of coupling constant α_s as :

$$X = \sum_{i=0}^N \alpha_s^n c_i = c_0 + \alpha_s^1 c_1 + \alpha_s^2 c_2 + \dots \quad (2.8)$$

where c_i are the perturbative coefficients. In a process, the pQCD calculation of X is determined by summing over the amplitudes of all Feynman diagrams contributing

of the gauge symmetry group $SU(3)_C$. The field tensor $F_{\mu\nu}^A$ is defined as

$$F_{\mu\nu}^A = \partial_\mu A_\nu^A - \partial_\nu A_\mu^A - g_s f_{ABC} A_\mu^B A_\nu^C$$

Summation implied
over identical indices
should be removed.

where g_s is the coupling constant determining the strength of the interaction between colored partons and f_{ABC} are the structure constants of the $SU(3)_C$ group. The last term in Eq. 2.3 is a non-abelian term which distinguishes QCD from QED and gives rise to a three- and a four-gluon vertex. In the term \mathcal{L}_{quarks} , $(D_\mu)_{ab}$ is the covariant derivative given by Eq. 2.4 and γ_μ are the Dirac γ -matrices.

$$(D_\mu)_{ab} = \partial_\mu \delta_{ab} + i g_s T_{ab}^A A_\mu^A \quad (2.4)$$

A_μ^A are the gluon fields with factors T_{ab}^A factors corresponding to the generators of the $SU(3)_C$ gauge group. The generators are represented via $T^A = \lambda^A/2$ by the Hermitian and traceless Gell-Mann matrices λ^A [16]. The generator matrices T^A follow the commutation relations :

$$[T^A, T^B] = i f_{ABC}^{\text{sum}} T^C \quad (2.5)$$

In \mathcal{L}_{QCD} , the classical contribution comes from \mathcal{L}_{gluons} and \mathcal{L}_{quarks} terms which give rise to the free quark- and gluon-field terms, and the quark-gluon interaction terms presented in Fig. 2.2. The cubic and quartic gluon self-interaction vertices proportional to g_s and g_s^2 , respectively, come into play due to the non-abelian property of QCD.

It is impossible to use perturbation theory on a gauge invariant Lagrangian without choosing a specific gauge in which to calculate. The usual gauge-fixing term

electromagnetic forces, respectively. $U(n)$ are the unitary and $SU(n)$ are the special unitary groups of degree n . The $SU(3)_C$ term defines the strong interaction between quarks and gluons mediated by gluons, with the three degrees of freedom of the color charge (C). The electromagnetic interaction of particles is explained by a well established modern theory called Quantum Electrodynamics (QED). In SM, the weak and electromagnetic interactions are combined by an electroweak symmetry theory, described by $SU(2)_L \otimes U(1)_Y$ gauge group. But this electroweak unification could not explain the occurrence of massive weak gauge bosons. This problem was solved by Brout-Englert-Higgs mechanism [10, 11]. The Higgs boson, named after Peter Higgs, is the field quantum of the Higgs field responsible for electroweak symmetry breaking. In SM, the Higgs field is a $SU(2)$ doublet which is a scalar under Lorentz transformations. The coupling of the bosons to the scalar Higgs field causes the spontaneous symmetry breaking which triggers the Higgs mechanism. After symmetry breaking, three of the four degrees of freedom in the Higgs field interact with the three weak gauge bosons (W^\pm and Z) and allows them to be massive, while the remaining one degree of freedom becomes the Higgs boson. Its existence was confirmed by the CMS [12] and ATLAS [13] collaborations in 2012, with the properties consistent with the SM. In contrast to the electroweak symmetry, the $SU(3)_C$ of the strong interaction is an exact symmetry and hence the gluons are massless. The strong interaction between quarks and gluons is described by theory called quantum chromodynamics (QCD), explained in detail in the next section.

2.2 Quantum Chromodynamics

The strong interactions between the quarks and gluons are described by a non-abelian gauge theory called quantum chromodynamics (QCD) [14, 15]. The gauge group of QCD is the special unitary group $SU(3)_C$ with color charges C as the generators of the gauge group. Color charge is the peculiar property of QCD and

~~fermions~~ need not be elementary. Nuclei are either fermions or bosons for example,

mental particles and the three of the four known ~~forces~~ of interactions between them, as summarized in Fig. 2.1. According to the SM, the basic constituents of matter are the elementary particles i.e. without any internal structure, known as fermions and bosons. The fermions have half integral spin and obey Fermi-Dirac statistics. They follow the Pauli exclusion principle according to which two or more identical fermions cannot occupy the same quantum state. Each fermion has an associated anti-particle having the same properties but opposite-sign quantum numbers.

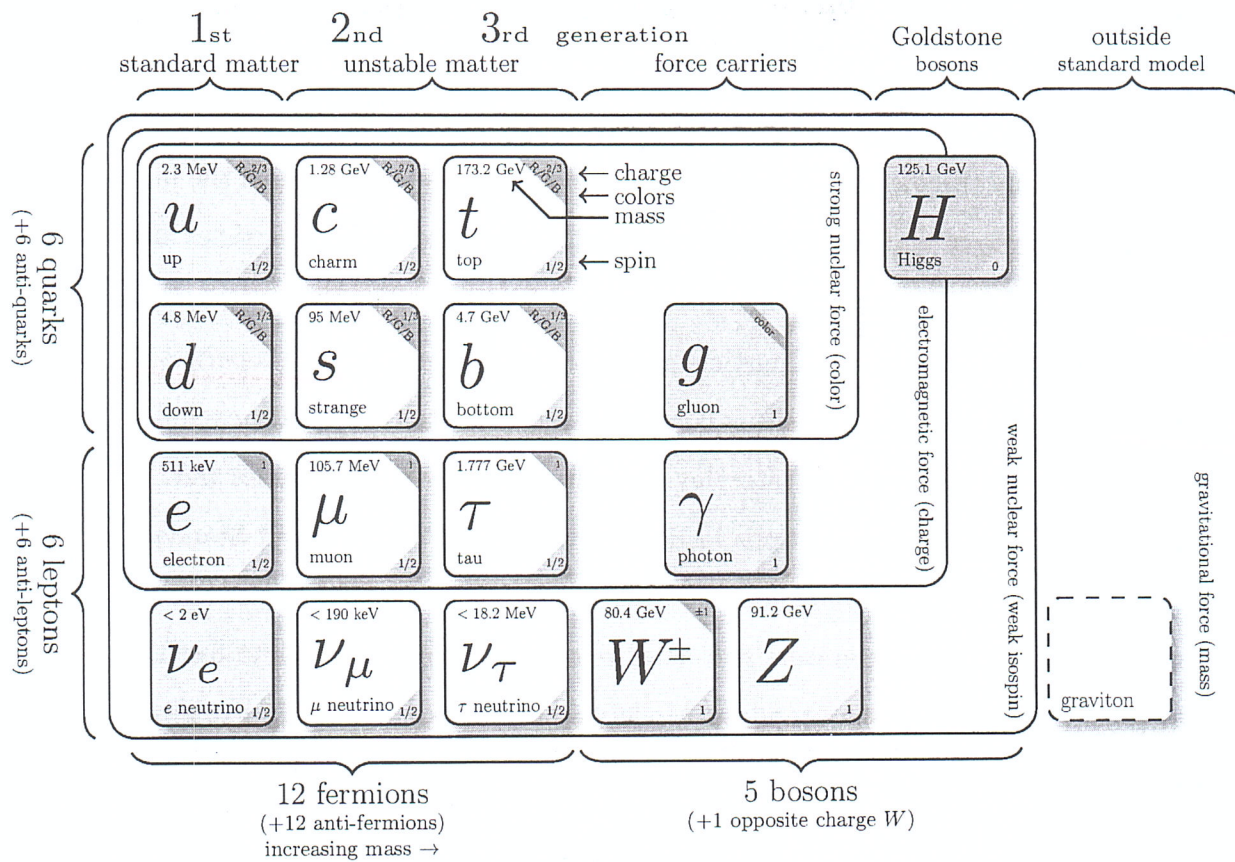


Figure 2.1: The Standard Model³ summarizing the properties of elementary particles known as fermions (leptons and quarks) grouped into three generations, gauge bosons as mediators for the interactions, the scalar Higgs boson and not incorporated graviton for the gravitational force.

³Source : <http://www.texample.net/tikz/examples/model-physics>

There are also 8 gluons...
if w^\pm are counted.

renormalization group equation (RGE)¹, which precisely describes the evolution of α_S ^{wifh} at the renormalization scale of QCD.

The organization of this thesis² is as follows :

Chapter 2 gives a brief overview of the Standard Model of particle physics and the theory of strong interactions QCD, theory of hadron collisions as well as formation of jets and jet algorithms.

Chapter 3 deals with experimental apparatus which covers the details of the geometry of the CMS detector and its various sub-detectors.

Chapter 4 describes the methods of event generation used in different Monte-Carlo event generators, detector geometry simulation and reconstruction of the particles in the detector. This chapter also gives the details of the different approaches of jet reconstruction at CMS and applied jet-energy corrections along with the description of the software framework used in the analysis presented in the current thesis.

Chapter 5 presents the measurement of differential inclusive multijet event cross-sections and the cross-section ratio. The measurements are corrected for detector effects by unfolding procedure which is discussed in detail in this chapter. The sources of the experimental uncertainties are studied in detail.

Chapter 6 contains a detailed description of the NLO perturbative QCD theory predictions obtained using different PDF sets. The NLO predictions are corrected with the non-perturbative and electroweak corrections. The theoretical uncertainties are calculated from various sources. At the end of this chapter, the unfolded measurements are compared with the predictions at NLO in pQCD as well as with the predictions from several Monte Carlo event generators.

¹According to the RGE, the strong force becomes weaker at short distances corresponding to large momentum transfers. This is referred to a property of QCD called asymptotic freedom.

²The common unit convention based on International System of Units (SI) as followed in particle physics will be used throughout the thesis. In addition, the units electron volt (eV) and barn (b) are used for energy and interaction cross-section, respectively. The reduced Planck constant (\hbar) and speed of light (c) are set to unity, i.e. $\hbar = c = 1$.

These data sets are analyzed in detail to reveal the structure and characteristic properties of the fundamental particles.

To search for the very rare particles, to investigate the physics beyond SM, and to explore the regime of undiscovered physical laws, the particle accelerators have become bigger and complex over the past few decades. The Large Hadron Collider (LHC) is one of the biggest and the most powerful particle collider in which the protons are accelerated and collided at extremely high center-of-mass energies to probe their internal structure and the parton distribution functions (PDFs). The PDFs give the probability to find a parton at an energy scale Q carrying a fractional momentum x of the proton. Since the proton is not elementary and is made up of partons, the proton-proton (pp) collisions are viewed as interactions between their constituent partons. The final products of the scattering are observed by Compact Muon Solenoid (CMS), one of the four detectors of the LHC, located around the interaction points of the collisions. The scattering cross-section can be expressed as a sum in terms of increasing powers of the strong coupling constant α_S convoluted with PDFs. The lowest-order α_S^2 term represents the production of two partons in final states whereas terms of higher-order α_S^3 , α_S^4 etc. signify the existence of multi-partons in final states. The highly energetic final state partons emit quarks and gluons with lower energies and give rise to a parton shower (PS). The colored products of parton shower hadronize to a spray of colorless hadrons known as jets. The jets are the final structures observed in the detector. So they carry the significant information of the energy and direction of the initial partons and hence are important to study. The final partons also have the probability to radiate more gluons and quarks which also hadronize and result in multijets in the final state. At LHC, such events are produced in large number and are an important source for testing the predictions given by QCD. They also serve as an important background in the searches for new particles and physics beyond SM.

The inclusive multijet event cross-section σ_{i-jet} , given by the process